# Geomechanical effects of carbon sequestration as $CO_2$ hydrates and $CO_2$-$N_2$ hydrates on host submarine sediments

*Shuman Yu*[1] and *Shun Uchida*[1,*]

[1]Department of Civil and Environmental Engineering, Rensselaer Polytechnic Institute, USA

**Abstract.** Over the past 10 years, more than 300 trillion kg of carbon dioxide ($CO_2$) have been emitted into the atmosphere, deemed responsible for climate change. The capture and storage of $CO_2$ has been therefore attracting research interests globally. $CO_2$ injection in submarine sediments can provide a way of $CO_2$ sequestration as solid hydrates in sediments by reacting with pore water. However, $CO_2$ hydrate formation may occur relatively fast, resulting decreasing $CO_2$ injectivity. In response, nitrogen ($N_2$) addition has been suggested to prevent potential blockage through slower $CO_2$-$N_2$ hydrate formation process. Although there have been studies to explore this technique in methane hydrate recovery, little attention is paid to $CO_2$ storage efficiency and geomechanical responses of host marine sediments. To better understand carbon sequestration efficiency via hydrate formation and related sediment geomechanical behaviour, this study presents numerical simulations for single well injection of pure $CO_2$ and $CO_2$-$N_2$ mixture into submarine sediments. The results show that $CO_2$-$N_2$ mixture injection improves the efficiency of $CO_2$ storage while maintaining relatively small deformation, which highlights the importance of injectivity and hydrate formation rate for $CO_2$ storage as solid hydrates in submarine sediments.

## 1 Introduction

$CO_2$ emission from burning fossil fuels and industry processing traps heat in the atmosphere, which has grown from 30.4 Gigatonnes (Gt) in 2010 to 33.3 Gt in 2019 resulting global concern of climate change [1]. With unbalanced high $CO_2$ concentration in the atmosphere, temperature could keep rising and cause global warming, which may change water cycle, melt glacier, increase the mean sea level, etc. [2]. Recent extreme weather patterns have been linked with $CO_2$ emission, and if true, this could end up a vicious circle as the increase in the energy use could result in more $CO_2$ emission and this in return could trigger greater energy consumption to accommodate extreme hot or cold weather [3]. Growing $CO_2$ emission combined with its long-stay nature in the atmosphere requires the process of capture and storage of $CO_2$ from the atmosphere.

Different $CO_2$ sequestration concepts are brought up including $CO_2$ injection into deep geological formations of low permeability and carbon mineralization via reaction with metal oxides. Nevertheless, the former may involve leakage issue due to the mobility of $CO_2$ fluid and the latter usually requires long time for producing stable carbonates, thus limiting $CO_2$ storage efficiency [4].

Gas hydrate formation in marine sediments provides a promising way of sequestering $CO_2$ in solid phase [5], effectively reducing the possibility of $CO_2$ escape from storage reservoir. When injected $CO_2$ is mixed with free water in marine sediments, $CO_2$ hydrates can form under suitable conditions of pressure and temperature. $CO_2$ hydrates are ice-like solids enclosing $CO_2$ molecules within the lattice cage of water molecules. Studies on $CO_2$ hydrate kinetics found relatively fast formation rate of $CO_2$ hydrates [6]. As gas hydrates grow rapidly in the pore space of marine sediments, the permeability can be largely reduced and thus adversely affect the $CO_2$ injectivity and transportation. In response, $N_2$ is suggested as an additive to reduce the rate of hydrate formation [7-9]. This is because $N_2$ hydrate is less thermodynamically stable and hence the mixed $N_2$ and $CO_2$ can propagate further into the sediments. However, these studies seldomly consider $CO_2$ storage efficiency and little attention is paid to deformation of the sediment and its effect on fluid flow.

To investigate gas hydrate-based carbon storage efficiency and associated geomechanical response, this paper presents two cases of pure $CO_2$ injection and $CO_2$-$N_2$ mixture (90-10 mol%) injection into water saturated marine sediments. The following section describes new components of hydrate mixture and fluid mixture that are required to capture behaviour of $CO_2$-$N_2$ hydrate mixture. Next, model geometry and the initial conditions are presented before discussing the advantage of $CO_2$-$N_2$ mixture injection in detail.

## 2 Equations for $CO_2$-$N_2$ fluid mixture and hydrate mixture in sediments

$CO_2$ and $N_2$ injection in marine sediments could lead to the generation of $CO_2$-$N_2$ fluid mixture and hydrate

* Corresponding author: uchids@rpi.edu

© The Authors, published by EDP Sciences. This is an open access article distributed under the terms of the Creative Commons Attribution License 4.0 (http://creativecommons.org/licenses/by/4.0/).

mixture (via reacting with free water). Built on the coupled thermo-hydro-chemo-mechanical formulation for single gas and hydrate developed by Klar et al. [10], equations are implemented for $CO_2$ and $N_2$ components including fluid mixture flow, diffusion of fluid mixture and partial pressure-based hydrate mixture formation.

Mass storage of $CO_2$ and $N_2$ in marine sediments is related to $CO_2$-$N_2$ fluid mixture flow, diffusion and hydrate reaction. The flow of $CO_2$-$N_2$ fluid mixture is governed by the Darcy's law, similar to conventional two-phase flow such that water being wet fluid and $CO_2$-$N_2$ mixture being dry fluid. The density of dry fluid consists of both $CO_2$ and $N_2$, which is defined as:

$$\rho_f = \rho_{cf} + \rho_{nf} \quad (1)$$

where $\rho$ is density and subscripts *f*, *cf* and *nf* denotes fluid mixture, $CO_2$ fluid and $N_2$ fluid, respectively. Diffusion of $CO_2$ and $N_2$ within the dry fluid mixture, caused by difference in molar concentration, is determined by Fick's law:

$$\boldsymbol{j}_{cf} = -D_{cf}\boldsymbol{\nabla} x_{cf} \quad (2)$$

$$\boldsymbol{j}_{nf} = -D_{nf}\boldsymbol{\nabla}(-x_{cf}) \quad (3)$$

where $\boldsymbol{j}$ and $\boldsymbol{\nabla}$ are diffusive flux and vector differential operator, respectively, $D$ is diffusion coefficient, and $x_{cf}$ is the molar fraction of $CO_2$ in the dry fluid mixture. When single $CO_2$ or $N_2$ fluid is injected into marine sediment, $CO_2$ hydrates or $N_2$ hydrates can form under suitable pressure and temperature conditions (as shown in Fig. 1). The difference between hydrate equilibrium pressure and fluid pressure drives single hydrate formation. When $CO_2$-$N_2$ fluid mixture is present with free water, partial pressure difference between fluid phase and hydrate phase is assumed to govern the hydrate reaction of each component. In ideal fluid mixture, the partial pressure is given by:

$$P_{cf} = x_{cf}P_f \quad (4)$$

$$P_{nf} = (1 - x_{cf})P_f \quad (5)$$

where $P$ is fluid pressure. Partial hydrate equilibrium in a homogeneous solution is given by Chen and Guo [11]:

$$P_{ch}^{eq} = x_{ch}P_{ch}^{eq0} \quad (6)$$

$$P_{nh}^{eq} = (1 - x_{ch})P_{nh}^{eq0} \quad (7)$$

where $P^{eq}$ is partial equilibrium hydrate equilibrium of $CO_2$ or $N_2$ in hydrate mixture and $P^{eq0}$ is pure $CO_2$ or $N_2$ hydrate equilibrium, $x_{ch}$ is molar fraction of $CO_2$ in hydrate mixture, and subscripts *ch* and *nh* denote $CO_2$ hydrate and $N_2$ hydrate, separately. The rate of hydrate reaction for each component is then given as:

$$R_{ch} = nS_g K_{ch}^f A_{ch}^s \langle P_{cf} - P_{ch}^{eq} \rangle - nS_{ch} K_{ch}^d A_{ch}^s \langle P_{ch}^{eq} - P_{cf} \rangle \quad (9)$$

$$R_{nh} = nS_g K_{nh}^f A_{nh}^s \langle P_{nf} - P_{nh}^{eq} \rangle - nS_{nh} K_{nh}^d A_{nh}^s \langle P_{nh}^{eq} - P_{nf} \rangle \quad (10)$$

where $\langle\cdot\rangle$ is Macaulay bracket, $n$ is porosity, $S$ is saturation, $K^f$ is hydrate formation constant, $K^d$ is hydrate dissociation constant, and $A^s$ is hydrate surface area per unit hydrate volume. The parameters for $CO_2$ and $CH_4$ hydrates are listed in Table 1. Note that since the intrinsic formation and dissociation rate of $N_2$ hydrates are not available from published reports, both are assumed to be same as $CO_2$ hydrates in this simulation.

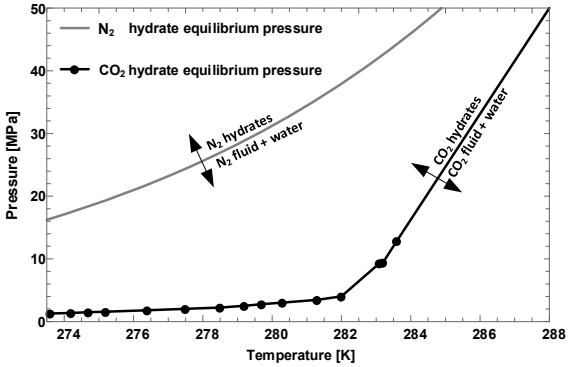


**Fig. 1.** Equilibrium pressure for single $CO_2$ hydrate and $N_2$ hydrate [12-13].

**Table 1.** $CO_2$ and $N_2$ hydrate parameters.

| | **$CO_2$ hydrate*** | **$N_2$ hydrate** |
|---|---|---|
| Density ($g/cm^3$) | 1.1 | 0.98 |
| Hydrate number | 6 | 6 |
| $P^{eq0}$ (kPa) | $e^{(45.02-10317/T)}$, $T$<283.15 K<br>$e^{(253.04-68865/T)}$, $T$>283.15 K | $e^{(37.808-7688.63/T)}$ [13] |
| Enthalpy (kJ/mol) | 208-0.53$T$ | 25.89+0.0769$T$ [13] |
| Formation constant ($mol/m^2/Pa/s$) | $4.8\times10^{-9}$ | $4.8\times10^{-9}$ |
| Dissociation constant ($mol/m^2/Pa/s$) | $1.8\times10^{8}\, e^{-12376/T}$ | $1.8\times10^{8}\, e^{-12376/T}$ |
| Surface area (1/m) | $0.375\times10^{-6}$ | $0.375\times10^{-6}$ |
| Specific heat (J/g/mol) | 2.01 | 2.13 |
| Thermal conductivity (W/m/K) | 0.49 | 0.5 |
| Thermal expansion (1/K) | $2.3*10^{-4}$ | $0.6*10^{-4}$ |

*$CO_2$ hydrate parameters are same as used in Deusner et al. [14] and Uchida et al. [15].

Combining the above three processes, incremental mass change of $CO_2$ or $N_2$ is obtained as:

$$dm_{cf} = -\nabla \cdot (\rho_{cf}\mathbf{q}_f)\mathrm{d}t - \nabla(\rho_{cf}D_{cf}\nabla x_{cf})dt - M_{cf}R_{ch}dt \quad (11)$$

$$dm_{nf} = -\nabla \cdot (\rho_{nf}\mathbf{q}_f)\mathrm{d}t + \nabla(\rho_{nf}D_{nf}\nabla x_{cf})dt - M_{nf}R_{nh}dt \quad (12)$$

where $\mathbf{q}_f$ is flow flux vector of $CO_2$-$N_2$ gas mixture governed by Darcy's law, $t$ is time, $M$ is molecular mass, $R$ is hydrate formation ($R$>0) or dissociation rate ($R$<0). Similarly, equations of incremental water and hydrates mass can be obtained. Finally, taking into account the saturation summation in the pore space and capillary pressure between water and fluid mixture, incremental pressure, saturation and temperature can be derived, which are related to coupled processes of heat transfer, fluid flow and diffusion, hydrate reaction and mechanical deformation during gas hydrate formation of injected $CO_2$ and $CO_2$-$N_2$ in sediments. These are not expanded in this paper and please refer to the mentioned literature for reference.

## 3 Model description

Two cases are considered in this study: Case I is $CO_2$ injection and Case 2 is $CO_2$-$N_2$ mixture (90-10 mol%) injection. Fig. 2 presents an axisymmetric marine sediment model adopted in this study. The sediment model locates from 770 m to 850 m below sea level and from 230 m to 310 m below sea floor. At the top boundary, constant pore water pressure and effective vertical stress 7.7 MPa and 2.3 MPa, respectively, are applied. The vertical and horizontal effective stress are assumed to be equal, equivalent to the in-situ earth pressure coefficient of $K_0$ = 1.0. The bottom boundary is mechanically fixed with the constant pore water pressure being 8.5 MPa. From the top to the bottom, the temperature changes from 278 K to 281 K with a thermal gradient of 0.04 K/m. The injection well is arranged in the middle of the model between 807.5 m and 812.5 m and $CO_2$ and $CO_2$-$N_2$ are injected at the constant injection pressure of 8.6 MPa. At the far-field boundary, temperature, pore water pressures and effective stress are set to keep constant.

Initial intrinsic permeability is $10^{-13.5}$ m$^2$ with the horizontal permeability (=$10^{-13}$m$^2$) being 10 times of the vertical permeability (=$10^{-14}$m$^2$). When injected $CO_2$ and $CO_2$-$N_2$ form gas hydrates in marine sediments, the sediment permeability reduces and is considered to follow the permeability model of hydrate-bearing sediment $K_h$=$K(1-S_h)^N$ [16] with N being assumed as 5.74 in this study. The geomechanical behaviour of sediments is modelled by the methane hydrate critical state model [17], which considers the effect of hydrate contribution through hydrate-dependent strength, stiffness and dilatancy. In this study, the sediments around the well is subjected to unloading and its volumetric behaviour is presented in Fig. 3. For simplicity, this study assumes that $CO_2$ hydrate-bearing sediments and $CO_2$-$N_2$ hydrate-bearing sediments have the same geomechanical properties.

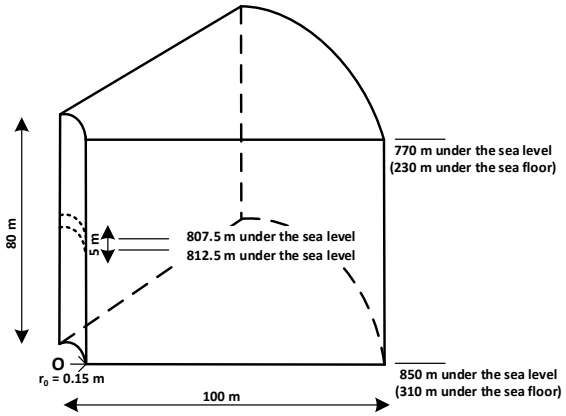


**Fig. 2.** Axisymmetric model of the marine sediment layer.

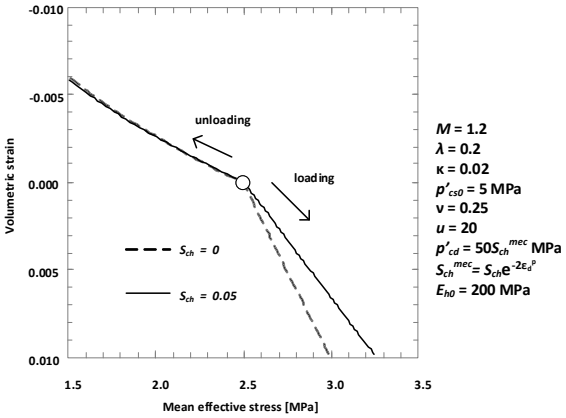


**Fig. 3.** Near-well sediment behaviour under isotropic loading.

## 4 $CO_2$ storage in marine sediments and geomechanical responses

Fig. 4 presents pore pressure profile of $CO_2$ injection for both Case I and Case II at t = 4 months. As the injection pressure is only 500 kPa greater than the initial pore pressure, the effect of pore pressure changes appears to be limited within the vicinity of well. However, the injected fluid travels much further than it appears from Fig. 4, and it forms $CO_2$ hydrate by reacting with pore water as shown in Fig. 5. Since injected fluid has lower density than the water, it tends to migrate upwards. In addition, due to lower temperature, upper area has more favourable condition for $CO_2$ hydrate formation and therefore greater amount of $CO_2$ hydrate forms in the upper area. Comparing between Case I and Case II, due to higher concentration of $CO_2$ in the injected fluid, higher $CO_2$ hydrate saturation is evident in Case I (Fig. 5a). This is also noticeable by higher temperature in Fig. 6, as $CO_2$ hydrate formation is exothermic process, implying that Case I forms a greater amount of hydrate near the well. However, because of higher $CO_2$ hydrate saturation, Case I eventually decreases injectivity due to reduction in the permeability. This is shown in Fig. 7. As a result, Case I has a slightly smaller region that injected fluid has propagated, resulting in lower $CO_2$ storage.

In order to highlight the effect of permeability reduction on $CO_2$ storage, Fig. 8 shows the development of overall amount of $CO_2$ stored as hydrate over a period of 4 months. As can be seen, although Case II has lower concentration of $CO_2$, Case II achieves a greater amount of $CO_2$ storage. In terms of geomechanical behaviour, Fig. 9 shows the development of averaged vertical strains (negative denotes extension) in the vicinity of injection zone, in specific, between r = 0.15 m and r = 1 m in radius and between z = 807.5 m and 812.5 m in depth. Because injection of fluid induces increase in the pore pressure, it induces vertical extension strain, implying heave of the sediments. Comparing the two cases, there is no significant difference and thus Case II has a greater advantage for geomechanical stability at a given amount of $CO_2$ storage. It is interesting to note that the heave occurs almost immediately after fluid injection, but with time, the sediment slowly compresses, which can be seen by the increase in the vertical strain. This is caused by the slow process of $CO_2$ hydrate formation as shown in Fig. 10, which presents the development of $CO_2$ hydrate in the vicinity of the injection well. Since the volume of water and $CO_2$ fluid required to form $CO_2$ hydrate is larger, hydrate formation reduces pore pressure. This increases the effective stress and thus the sediment compresses. The slow process of $CO_2$ hydrate formation is caused by the limited heat transfer. Since the injection pressure is constant, for $CO_2$ hydrate to keep forming, it needs to lower temperature. Under this condition, the temperature reduction can only occur by conduction, which is relatively slow process. Nonetheless, the trend of the results implies that $CO_2$ hydrate can keep forming while reducing the heave, which may help to achieve permanent $CO_2$ storage with geomechanically-stable method, especially when mixture of $CO_2$ and $N_2$ is injected.

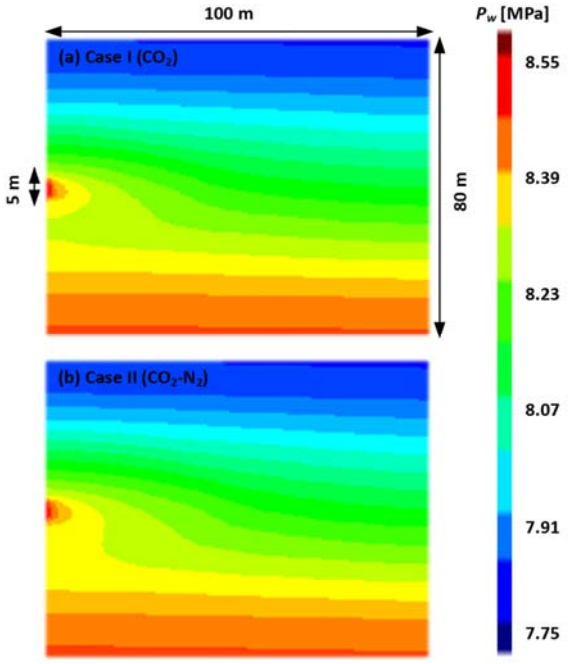


**Fig. 4.** Pore water pressure at 4 months for (a) Case I: $CO_2$ injection and (b) Case II: $CO_2$ and $N_2$ injection.

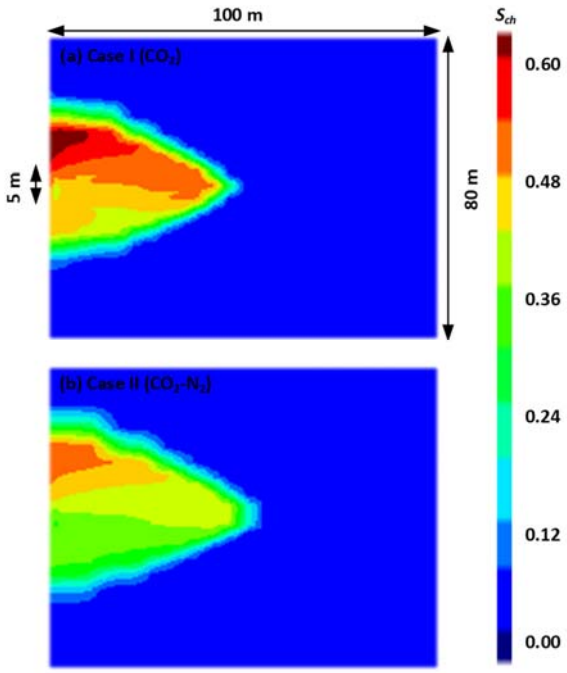


**Fig. 5.** $CO_2$ hydrate saturation at 4 months for (a) Case I: $CO_2$ injection and (b) Case II: $CO_2$ and $N_2$ injection.

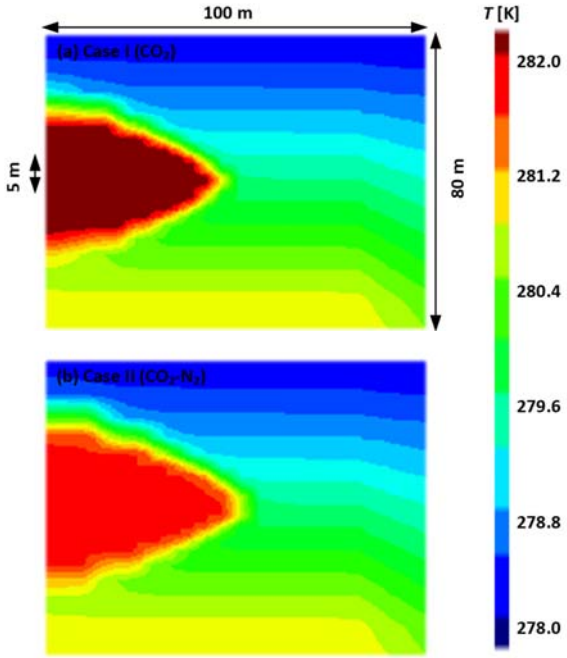


**Fig. 6.** Temperature at 4 months for (a) Case I: $CO_2$ injection and (b) Case II: $CO_2$ and $N_2$ injection.

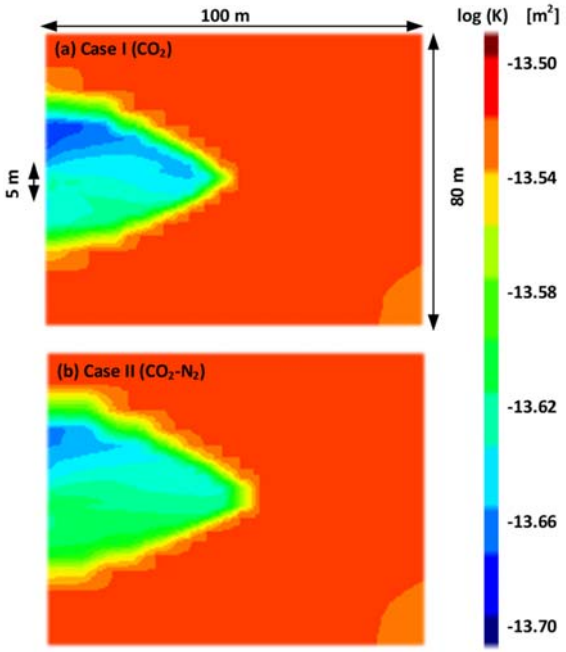


**Fig. 7.** Permeability at 4 months for (a) Case I: $CO_2$ injection and (b) Case II: $CO_2$ and $N_2$ injection.

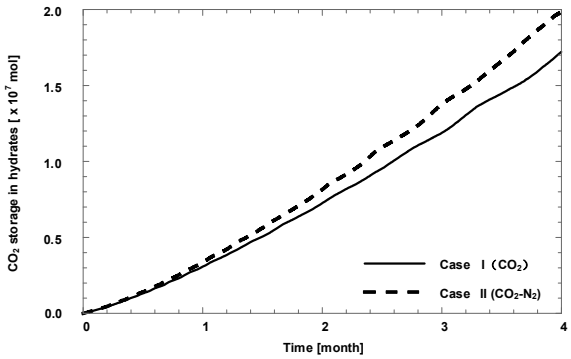


**Fig. 8.** $CO_2$ storage as solid hydrates during 4-month injection for (a) Case I: $CO_2$ injection and (b) Case II: $CO_2$ and $N_2$ injection.

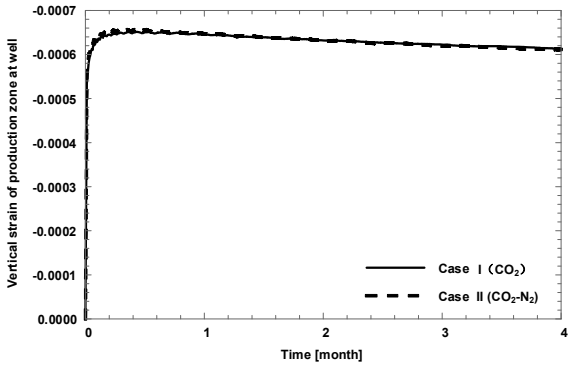


**Fig. 9.** Vertical strain of 5-m injection zone at the well during 4-month injection for (a) Case I: $CO_2$ injection and (b) Case II: $CO_2$ and $N_2$ injection.

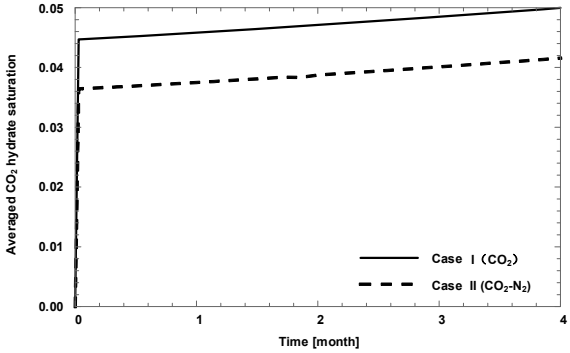


**Fig. 10.** Averaged $CO_2$ hydrate saturation of 5-m injection zone at the well during 4-month injection for (a) Case I: $CO_2$ injection and (b) Case II: $CO_2$ and $N_2$ injection.

## 5 Conclusions

$CO_2$ storage can be achieved by formation of solid hydrates in marine sediments. To consider the $CO_2$ storage efficiency and geomechanical response of host sediments, two cases of $CO_2$ and $CO_2$-$N_2$ injection (90-10 mol%) into marine sediment are simulated with the implementation of gas mixture and hydrate mixture in the coupled formulation. Three key findings as of 4-month injection are presented below:

- $CO_2$-$N_2$ injection case has more $CO_2$ amount being sequestered as hydrates in marine sediments due to moderate reduction of permeability from relatively slow $CO_2$-$N_2$ hydrate mixture formation.
- Vertical extension near the well is observed immediately after fluid injection in both cases because of increased pore pressure.
- Vertical strain near the well then gradually decreases as $CO_2$ hydrate forms which depends on heat transfer.

Although this study considers only one pressure-temperature condition, the favourable effects of $CO_2$-$N_2$ injection on geomechanical stability and $CO_2$ storage efficiency are likely to stand for different pressure and temperature of marine setting as $N_2$ hydrate remains less stable. The preliminary finding is promising, and future study includes the effect of different concentrations of the $CO_2$-$N_2$ mixture.

## References

1. IEA, https://www.iea.org/articles/global-co2-emissions-in-2019 (accessed 5 March 2020)
2. IPCC, *Summary for Policymakers. In: Climate Change 2013: The Physical Science Basis* (Cambridge University Press, Cambridge, UK and New York, NY, USA, 2013)
3. BP, *BP Statistical Review of World Energy* (London, 2019)
4. IPCC, *IPCC Special Report on Carbon Dioxide Capture and Storage* (Cambridge University Press, Cambridge, UK and New York, NY, USA, 2005)

5. K. Ohgaki, Y. Inoue, *A Proposal for Gas Storage on The Bottom of The Ocean Using Gas Hydrates*, Int. Chem. Eng. **34**, 417-419 (1994)
6. E.D. Sloan, C.A. Koh, *Clathrate Hydrates of Natural Gases, 3rd Edition* (Taylor & Francis/CRC Press, Boca Raton, 2008)
7. G. Ersland, J. Husebø, A. Graue, B. Kvamme, *Transport and Storage of $CO_2$ in Natural Gas Hydrate Reservoirs*, Energy Procedia, **1**, 3477-3484 (2009)
8. B. Kvamme, A. Graue, T. Buanes, T. Kuznetsova, G. Ersland, *Storage of $CO_2$ in Natural Gas Hydrate Reservoirs and the Effect of Hydrate as An Extra Sealing in Cold Aquifers*, Int. J. Greenh. Gas Con., **1**, 236-246 (2007)
9. B. Kvamme, *Feasibility of Simultaneous $CO_2$ Storage and $CH_4$ Production from Natural Gas Hydrate Using Mixtures of $CO_2$ and $N_2$*, Can. J. Chem., **93**, 897-905 (2015)
10. A. Klar, S. Uchida, K. Soga, K. Yamamoto, *Explicitly Coupled Thermal Flow Mechanical Formulation for Gas-Hydrate Sediments*, SPE, **18**, 196-206 (2013)
11. G. Chen, T. Guo, *Thermodynamic Modeling of Hydrate Formation Based on New Concepts*, Fluid Ph. Equilibria, **122**, 43-65 (1996)
12. S. Fan, G. Chen, Q. Ma, T. Guo, *Experimental and Modeling Studies on The Hydrate Formation of $CO_2$ and $CO_2$-Rich Gas Mixtures*, Chem. Eng. J., **78**, 173-178 (2000)
13. V.A. Kamath, *Study of Heat Transfer Characteristics during Dissociation of Gas Hydrates in Porous Media* (Ph.D. dissertation, University of Pittsburgh, 1984)
14. C. Deusner, N. Bigalke, E. Kossel, M. Haeckel, *Methane Production from Gas Hydrate Deposits through Injection of Supercritical $CO_2$*, energies, **5**, 2112-2140 (2012)
15. S. Uchida, C. Deusner, A. Klar, M. Haeckel, *Thermo-Hydro-Chemo-Mechanical Formulation for CH4-CO2 Hydrate Conversion Based on Hydrate Formation and Dissociation in Hydrate-Bearing Sediments*, Geo-Chicago 2016 (2016)
16. Y. Masuda, S. Naganawa, K. Fujita, K. Sato, Y. Hayashi, *Modeling and Experimental Studies on Dissociation of Methane Gas Hydrates in Berea Sandstone Cores*, ICGH3 (1999)
17. S. Uchida, K. Soga, K. Yamamoto, *Critical State Soil Constitutive Model for Methane Hydrate Soil*, J. Geophys. Res. Solid Earth, **117** (2012)